Colloids and Surfaces B: Biointerfaces 115 (2014) 244–252

Contents lists available at ScienceDirect

Colloids and Surfaces B: Biointerfaces

journal homepage: www.elsevier.com/locate/colsurfb

Antibacterial and wound healing analysis of gelatin/zeolite scaffolds

Neethu Ninan[a,b,*], Muthunarayanan Muthiah[c], Nur Aliza Bt.Yahaya[d], In-Kyu Park[c], Anne Elain[a], Tin Wui Wong[d], Sabu Thomas[b], Yves Grohens[a]

[a] Université de Bretagne Sud, Laboratoire Ingénierie des Matériaux de Bretagne, BP 92116, 56321 Lorient Cedex, France
[b] Centre for Nanoscience and Nanotechnology and School of Chemical Sciences, Mahatma Gandhi University, Priyadarsini Hills PO, Kottayam 686 560, Kerala, India
[c] Department of Biomedical Science and BK21 PLUS Center for Creative Biomedical Scientists, Chonnam National University Medical School, 160 Baekseo-ro, Gwangju 501-746, Republic of Korea
[d] Non-Destructive Biomedical and Pharmaceutical Research Centre, Universiti Teknologi MARA, 42300 Puncak Alam, Selangor, Malaysia

ARTICLE INFO

Article history:
Received 29 July 2013
Received in revised form
25 November 2013
Accepted 26 November 2013
Available online 4 December 2013

Keywords:
Gelatin
Copper activated faujasite
Anti-bacterial
Wound healing
Animal studies
Fibroblast

ABSTRACT

In this article, gelatin/copper activated faujasites (CAF) composite scaffolds were fabricated by lyophilisation technique for promoting partial thickness wound healing. The optimised scaffold with 0.5% (w/w) of CAF, G (0.5%), demonstrated pore size in the range of 10–350 μm. Agar disc diffusion tests verified the antibacterial role of G (0.5%) and further supported that bacterial lysis was due to copper released from the core of CAF embedded in the gelatin matrix. The change in morphology of bacteria as a function of CAF content in gelatin scaffold was studied using SEM analysis. The confocal images revealed the increase in mortality rate of bacteria with increase in concentration of incorporated CAF in gelatin matrix. Proficient oxygen supply to needy cells is a continuing hurdle faced by tissue engineering scaffolds. The dissolved oxygen measurements revealed that CAF embedded in the scaffold were capable of increasing oxygen supply and thereby promote cell proliferation. Also, G (0.5%) exhibited highest cell viability on NIH 3T3 fibroblast cells which was mainly attributed to the highly porous architecture and its ability to enhance oxygen supply to cells. *In vivo* studies conducted on Sprague Dawley rats revealed the ability of G (0.5%) to promote skin regeneration in 20 days. Thus, the obtained data suggest that G (0.5%) is an ideal candidate for wound healing applications.

Crown Copyright © 2013 Published by Elsevier B.V. All rights reserved.

1. Introduction

Wound infections are caused due to invasion of injured tissues by microorganisms, that trigger body's immune system, induce inflammation, tissue damage and impede the healing process [1]. Most cases of infected wounds arise due to bacteria, originating either from the skin or external environment [2]. Skin contains normal flora of bacteria which are harmless. When it is subjected to injury, this protective barrier will be disrupted and the normal flora will then colonise the wounded site, inducing inflammation and tissue damage, thereby causing serious local and systemic complications [3]. One of the approaches for treating bacterial infected wounds is the use of biocompatible scaffolds incorporated with antibacterial agents [4]. Several polymers are used for the fabrication of such scaffolds including pectin [5], chitin [6], chitosan [7], alginate [8], collagen [9], gelatin [10], keratin [11], polyurethane [12], polycaprolactone [13], polyacrylonitrile [14], polyethylene [15] and silicon rubber [16]. Among these, gelatin is chosen as a suitable matrix due to its natural abundance, biocompatibility, biodegradability and non-immunogenicity [17]. It is a protein obtained by partial hydrolysis of collagen. It melts into liquid when heated and gets solidified when cooled [18]. Literature reports the wide use of gelatin in preparing scaffolds with antibacterial properties like electrospun gelatin fibre mats containing silver nanoparticles [19], keratin-gelatin composites [20], chitosan-gelatin/nanohydroxyapatite scaffold [21], electrospun chitosan/gelatin nanofibers containing silver nanoparticles [22], gelatin/hydroxyapatite foams [23], nanosilver/gelatin/carboxymethyl chitosan hydrogel [24], *etc.* We prepared scaffolds with antibacterial properties using gelatin as the polymer matrix.

Recently, inorganic minerals like clays and zeolites containing metals have achieved great significance compared to conventional antibacterial agents. The incorporation of metallic ions within silicate framework allowed their controlled release and prevented concentration dependent toxicity [25]. Among the different inorganic materials, copper containing minerals are prominent as

* Corresponding author at: Université de Bretagne-Sud, Laboratoire d'Ingénierie des MATériaux de Bretagne (LIMatB), Centre de Recherche Christiaan Huygens, Rue de St Maudé – BP 92116, Bureau 32 bis, 56321 Lorient Cedex, France.
Tel.: +33 751464109/+91 0484 2557031; fax: +33 02 97 87 45 19.
E-mail address: neethuninan85@yahoo.co.in (N. Ninan).

0927-7765/$ – see front matter. Crown Copyright © 2013 Published by Elsevier B.V. All rights reserved.
http://dx.doi.org/10.1016/j.colsurfb.2013.11.048

copper ions can stimulate the proliferation of endothelial cells, promote wound healing and exhibit broad spectrum of antibacterial properties [26]. In the present study, copper exchanged faujasite (CAF) were chosen as suitable antibacterial agent. They are mineral groups of zeolite family with excellent cation exchange ability. They consist of sodalite cages connected through hexagonal prisms, forming a large central cavity of diameter ~12 Å [27]. The inner cavity is linked to 12 membered rings of diameter ~7.4 Å [28]. Seifu et al., has reported that fluorinated zeolites embedded within polymeric scaffolds can enhance oxygen delivery to cells [29]. Besides the antibacterial property, our aim was to evaluate whether CAF can provide sufficient oxygen supply to the growing skin cells at wound site.

In this work, gelatin/CAF composite scaffolds were fabricated by lyophilisation and parameters like dissolved oxygen concentration, cumulative copper release, antibacterial properties and cytocompatibility were investigated. *In vivo* studies on Sprague Dawley rats were conducted to explore the wound healing ability of prepared composite scaffold.

2. Materials and methods

2.1. Materials

Type B gelatin, glycerol (purity-99%), formaldehyde (36.5–38%), glutaraldehyde (25%) and phosphate buffered saline (PBS) were purchased from Sigma–Aldrich (France). Zeolite powder (CAF) was a kind gift from IRMA (France). Mueller Hinton agar, Luria broth (LB), sodium chloride, absolute ethanol (100%), Dulbecco's modified Eagle Medium (DMEM), MTS reagent and sterile antibiotic discs (diameter-4 mm) were acquired from Sigma–Aldrich (France). 25% (v/v) ammonia, xylene and hydrochloric acid were obtained from Merck (Damstadt, Germany). The staining reagents like Harris haematoxylin and eosin were procured from Leica Biosystems Richmund Inc. (Germany). Ketamine hydrochloride and xylazine hydrochloride were bought from Troy Laboratories, Australia. *Escherichia coli* (ATCC 25922) were obtained from microbiology department of IUT, South Brittany (Pontivy, France). NIH 3T3 fibroblast cells were procured from ATCC cell biology collection.

2.2. Preparation of gelatin/CAF composite scaffold

Gelatin/CAF porous scaffolds were synthesised by lyophilisation as reported in our previous work [30]. A 2% (w/v) of gelatin solution in water (endotoxin-free) was mixed with 5% (v/v) of glycerol (plasticiser). 2.5% (w/v) of CAF suspension was sonicated for 30 min, added to gelatin solution and immediately cross-linked using 10 μL of formaldehyde (0.38%). The solution was well mixed and poured onto petri plates. They were pre-frozen at −20 °C and lyophilised in Christ Alpha 1–2 LD Plus Freeze Dryer. G (0%) was the control scaffold synthesised without CAF. G (0.5%), G (2.5%) and G (5%) were gelatin/CAF composite scaffolds prepared with 0.5%, 2.5% and 5% (w/v) of CAF. GN (0.5%) was the composite scaffold with 0.5% (w/v) of faujasite without any copper, which was prepared to confirm whether antibacterial activity was induced by copper released from faujasite core.

2.3. SEM analysis

The morphology of scaffolds was investigated by scanning electron microscope (SEM) (JEOL-2100, Kyoto, Japan). Thin sections of scaffold were cut using razor blade. They were gold sputtered by Polaron sputtering apparatus and examined under SEM.

2.4. Dissolved oxygen measurements

Hach luminescent dissolved oxygen electrode (LDO 101-01), equipped with 1 or 3 m cables was used to measure dissolved oxygen (DO) in CAF suspension. A light emitting diode transmitted incident light which was sufficient to excite the luminophore substrate. In the presence of DO, luminescence quenching took place. The dynamic lifetime of the excited luminophore was calculated and equated to DO concentration. CAF particles were suspended in deionised water at concentrations of 0.25%, 0.5%, 2.5%, 5% (w/v), respectively and continuously stirred at 37 °C. Deionised water was used as the control. The LDO probe was calibrated before use. The probe was partially submerged in CAF suspension and the reading was recorded. Triplicates of samples were done and average of the results was plotted.

2.5. Release characteristics of copper loaded in scaffolds

0.4 g of the prepared scaffold was weighed and placed on petri plates containing saline water [0.9% (w/v) of sodium chloride]. The plates were rotated on an orbital shaker at 150 rpm for 1 h at 37 °C. Samples were washed and saline water was replaced by fresh solution. The suspensions were centrifuged at 5000 × *g* for 5 min. The supernatants were collected and the concentration of Cu^{2+} ion was measured by Varian Spectra AA 600 atomic absorption spectroscopy (AAS) (Burladingen, Germany). Cumulative copper release from samples for six days were plotted and compared. All measurements were done in triplicates.

2.6. Antibacterial studies

In vitro antibacterial activity of the prepared scaffolds was quantitatively and qualitatively evaluated using disc diffusion method and live/dead assay technique. According to the recommended standards of National Committee for Clinical Laboratory Standards (NCCLS, 2005), agar disc diffusion method was carried out against *E. coli* (ATCC 25922), a gram negative bacterial strain. The samples analysed included the optimised scaffold, G (0.5%) and control scaffold without CAF, G (0%). Along with these samples, a disc of GN (0.5%) was also tested to check whether copper present in the faujasite was actually responsible for bacterial inhibition.

The suspensions of bacteria used for inoculation were prepared by adjusting fresh cultures at Mac Farland 0.5 density (approximately 10^8 CFU/ml). The inoculum was streaked on Mueller Hinton agar medium and then air dried at room temperature. The prepared scaffolds were cut in the form of small discs of diameter 4 mm and were placed on agar medium. Afterwards, the plates were incubated at 37 °C for 24 h. All tests were carried out in triplicates. Sterile paper discs about 4 mm in diameter, impregnated with Penicillin G, Pg (10 μg/disc) and Bactopin®, Bi (μL/disc) were used as positive controls. The antibacterial activity was calculated as the mean diameter of inhibition zones (mm) developed around the samples. Photographs were taken to further support these results.

In the live/dead assay technique, the samples were cut in the form of discs, diameter 6 mm and placed in the wells of microtiter plates containing 225 μL of LB broth and 25 μL of *E. coli* culture. The plates were kept in a shaking incubator at 37 °C. After 24 h, 100 μL of the sample was eluted and seeded onto agar medium. They were stained with DMAO and EthD-III and observed under confocal microscopy (Zeiss LSM 510, Germany), to determine the number of live or dead bacteria in the well.

2.7. Susceptibility tests

E. coli was cultured in LB broth at 37 °C for 24 h and was then diluted in fresh broth to reach the required optical density. A 2.5%

(v/v) glutaraldehyde solution was prepared in PBS (pH-7.4). About 1 mg sample each of G (0%), GN (0.5%), G (0.5%) and G (5%), was immersed separately in LB broth. To this, bacteria cultures were added and incubated at 37 °C for 24 h. Onto poly lysine coated glass slides, few drops of bacteria exposed to the samples were added and fixed using 2.5% glutaraldehyde. The glass slides were stored at 4 °C followed by washing the slides thrice, using PBS. Then, they were dehydrated using 70%, 96% and 100% (v/v) of absolute ethanol. The specimens were dried using EMS 850 critical point dryer and then gold sputtered for SEM analysis.

2.8. Cytocompatibility studies

The cytocompatibility of prepared scaffolds were evaluated using a colorimetric test named as MTS assay. The samples were cut into small pieces of equal weights and placed on 24 well plates. They were sterilised by overnight UV exposure. NIH 3T3 fibroblasts were cultured in Dulbecco's modified Eagle Medium with 10% FBS and 1% antibiotic at 37 °C in a humidified atmosphere with 5% CO_2. The cells were harvested and seeded on the scaffolds at a density of 5×10^4 cells/ml and incubated at 37 °C. After 48 h, MTS was added to the wells and further incubated for 4 h. Then the absorbance was measured at 495 nm using Microplate reader (Spectromax 180). Triplicates of samples were done and data was plotted as mean ± SD from which cell viability was evaluated.

2.9. In vivo studies

In vivo studies were conducted on six male Sprague Dawley rats purchased from Genetic Improvement and Farm Technologies Sdn Bhd Malaysia. The rats were acclimatised to laboratory conditions for 10 days before wounding. On the day of experiment (day 0), rats were given intramuscular injection of a mixture of 90 mg/kg of ketamine and 10 mg/kg of xylazine, as anaesthesia. The dorsal area of each rat was shaved and skin was wiped with 70% alcohol swab. A single round partial thickness wound was created on the back of each rat by adding 6 ml of hot deionised water at 80 °C, through a circular plastic ring, fastened to the dorsal area using adhesive glue, in 9 repetitive cycles. The wound was then dressed with prepared composite scaffold which showed highest cytocompatibility, using standard gauze and 3 M adhesive tape. The rats were housed in individual cages and maintained at a temperature of 25 ± 2 °C and humidity of 55 ± 2% with a HEPA filter system. Animals were divided into two groups, namely, Group 1 (control rats with untreated wounds) and Group 2 (rats treated with scaffolds). The rats were provided with deionised water and animal feed, during the post wounding period. The wounds were photographed and then redressed with composite scaffolds every day and the wound area was traced on a transparent polyethylene sheet. The size of wound was measured using digital micrometre (Mitutoyo, Japan). The percentage of wound area closure was evaluated using Eq. (1).

$$\text{Percentage of wound area closure } (\%) = 100 \times \frac{A_i - A}{A_i} \quad (1)$$

where A_i is the initial wound area calculated on day 0 and A is the wound area on day 't'.

2.10. Histochemistry

The rats were sacrificed on the twentieth day and the skin was excised, cleaned with isotonic saline solution, dried with clean cotton swab and stored at −20 °C in deep freezer. Using cryostat (Leica CM 1850 UV, Germany) the skin was cut into thin sections. Eight slices of skin of each sample were prepared and mounted on glass slides. They were stained by haematoxylin and eosin (H&E) staining reagents in Autostainer XL (Leica, Germany) and observed

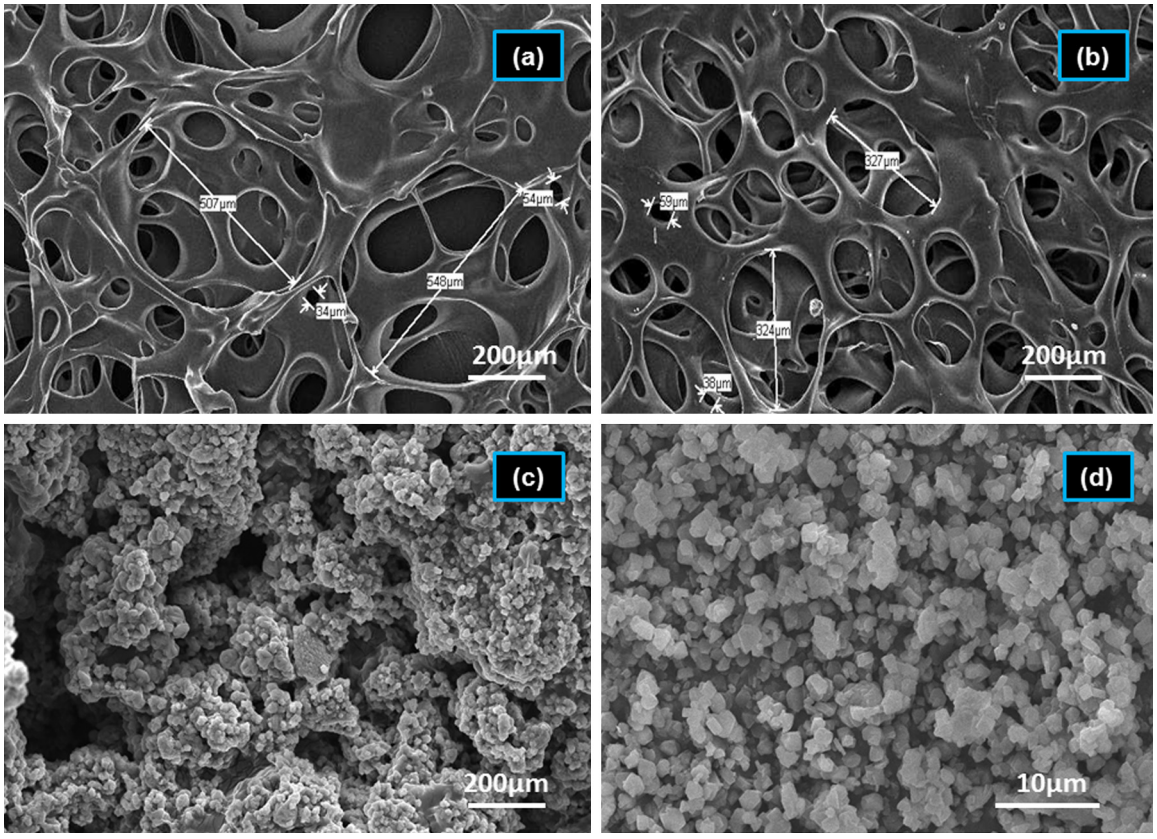

Fig. 1. SEM image of (a) G (0%), (b) G (0.5%), (c) G (5%) and (d) CAF particles.

under compound microscope (Leica DF2500, Germany), fitted with a camera to capture digital images of stained sections.

3. Results and discussion

3.1. SEM analysis

Fig. 1 showed the SEM images that make a distinction between the morphology of scaffolds prepared with low and high concentration of copper activated faujasites (CAF). In our previous paper, it was found that pore size of G (0%), was greatly reduced after the incorporation of 0.5% (w/v) of CAF in the gelatin matrix and this might be due to good reinforcing properties of CAF [30]. The control scaffold, G (0%) exhibited pore size in the range of 50–750 μm.

In this article, we were able to prove that higher concentration of CAF, the pore size was found to increase due to agglomeration of CAF particles leading to rugged surface compared to G (0.5%). The pore size of G (0.5%) was 10–350 μm and that of G (5%) was 10–550 μm. In case of G (0.5%), pores found in the range of 10–50 μm might aid in keratinocyte infiltration and 100–250 μm promoted fibroblast proliferation [31]. CAF particles had octahedral morphology which was a distinct feature of faujasites and these particles were found embedded in the composite scaffold.

3.2. Copper release studies

The framework of faujasite consists of quadri-charged silicon which was replaced by triply-charged aluminium, giving rise to deficit of positive ions. This inadequacy was balanced by copper ions giving rise to the structure of CAF [32]. The loosely bound copper cations could be easily exchanged when immersed in solution of saturating or indexing ions [32]. Each cation of copper could be exchanged with monovalent or divalent ions in solution. When CAF was dispersed in saline solution, ion exchange took place in which copper ions were replaced by sodium ions. The released copper was detected by atomic absorption spectroscopy (AAS). Fig. 2 indicated that with increase in time, release of copper increased and reached saturation, after 48 h. The amount of copper released in 24 h for G (0.5%), G (2.5%) and G (5%) were 0.9 ± 0.02 μg/ml, 5 ± 0.14 μg/ml and 11 ± 0.3 μg/ml, respectively. Around 1.4 ± 0.015 μg/ml of copper was leached from G (0.5%) after 6 days whereas higher amounts of copper were released from G (2.5%) and G (5%) which can prove to be lethal to mammalian cells. Liu et al., has reported about neurotoxicity induced by uptake of higher amount of copper drugs [33]. There are several reports that confirmed concentration dependent toxicity of copper. Thus, G (0.5%) was the suitable scaffold with optimum release of copper, to kill bacteria at wound site without imparting toxicity to normal skin cells.

3.3. Disc diffusion tests

The anti-bacterial properties of G (0%), GN (0.5%) and G (0.5%) were investigated against gram negative bacteria (*E. coli*). The results proved that G (0%) and GN (0.5%) did not show any antibacterial activity. GN (0.5%) with non-activated faujasites were tested to determine whether bacterial lysis was caused due to copper released from faujasites. A zone of inhibition was seen around G

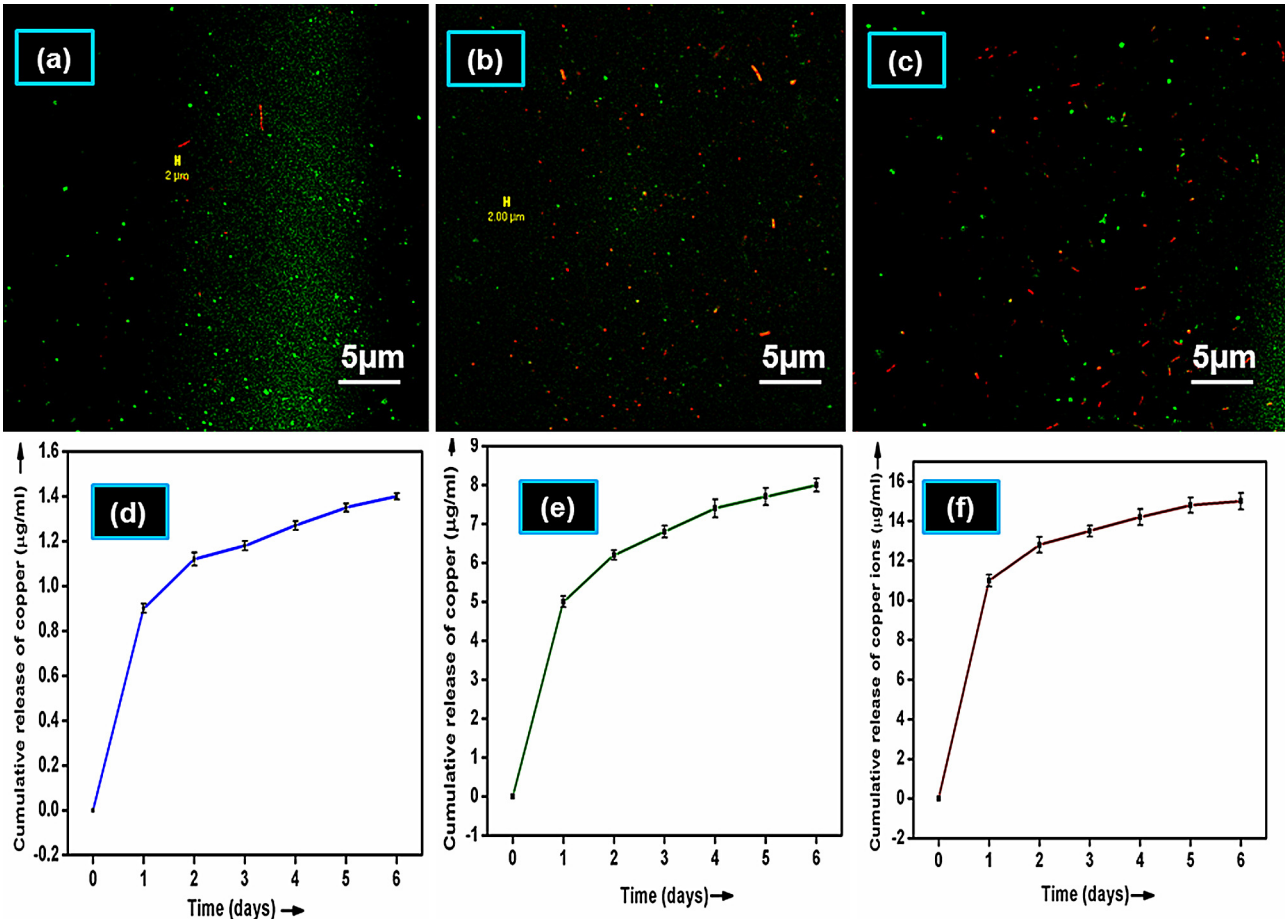

Fig. 2. Confocal microscope images of bacteria exposed to (a) G (0.5%), (b) G (2.5%) and (c) G (5%). Live bacteria were stained green and dead bacteria were stained red. Cumulative release of copper from (d) G (0.5%), (e) G (2.5%) and (f) G (5%). Values were expressed as mean ± SD ($n = 3$). (For interpretation of the references to color in this figure legend, the reader is referred to the web version of this article.)

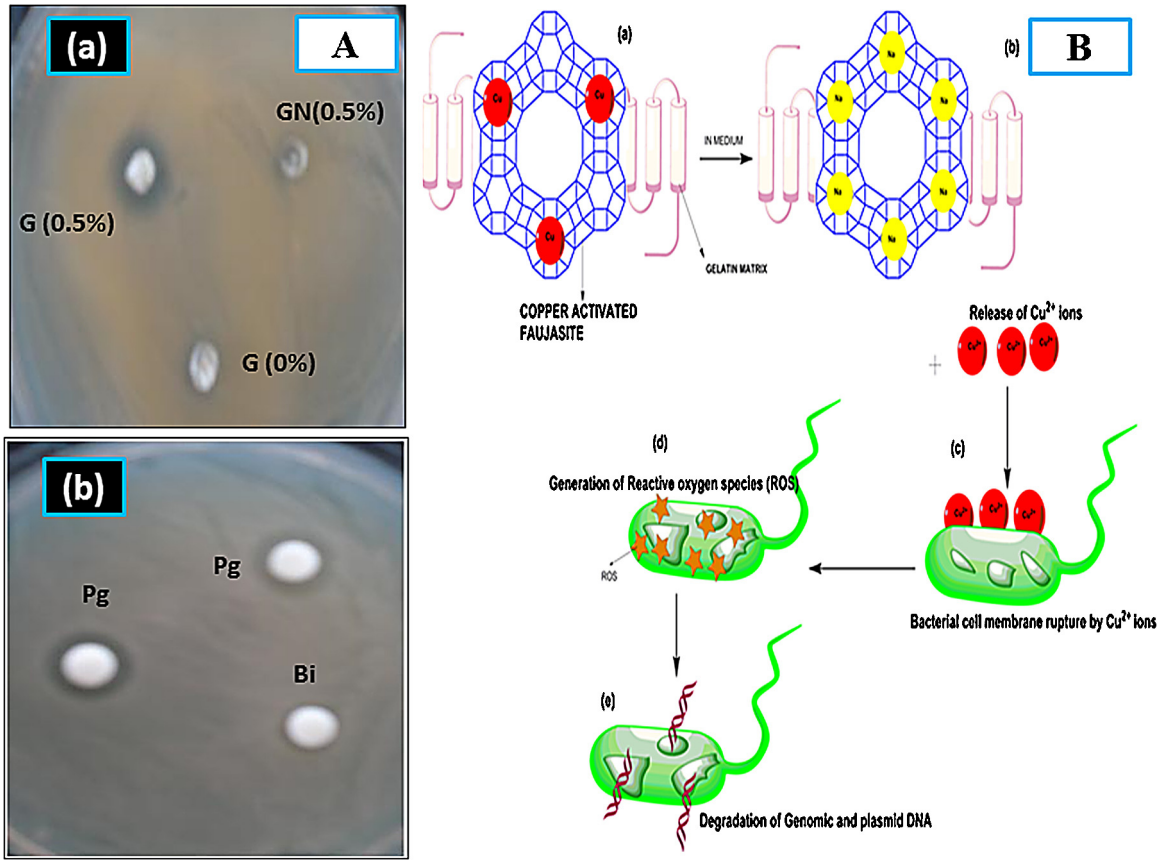

Fig. 3. (A) Agar disc diffusion tests of (a) G (0%), GN (0.5%), G (0.5%); (b) positive control discs, Pg and Bi against *Escherichia coli*. All tests were carried out in triplicates ($n = 3$). (B) Schematic diagram showing bacterial lysis by copper released from pore of CAF.

(0.5%), diameter 8.82 ± 0.28 mm. The positive control discs, Penicillin (Pg) and Bactopin® (Bi) showed inhibition zones of diameters 12.63 ± 0.3 mm and 9.26 ± 0.2 mm respectively (Fig. 3A). Inhibition zone was the area around the disc where bacteria would not survive as they were susceptible to the antibacterial agents that diffused from the sample to the surrounding medium [34]. The data ascertained that G (0.5%) showed significant bacterial lysis.

Representative images of bacterial live/dead assay were shown in Fig. 2(a–c) for samples treated with *E. coli*. In this assay, two nucleic acid dyes were used namely, DMAO and EthD-III. DMAO was a green fluorescent dye that stained both live and damaged cell membranes whereas red coloured EthD-III stained dead bacteria. Thus, live cells appeared green and red colour denoted dead cells. Fig. 2a demonstrated that mortality rate of bacteria exposed to G (0.5%) was moderate. On the other hand, G (5%) showed the highest mortality rate. This further supported the argument that bacterial lysis was caused by copper released from CAF and its effect increased with increase in the concentration of CAF present in the composite matrix.

A probable mechanism for the bactericidal activity of G (0.5%) was shown in Fig. 3B. When the composite scaffold was placed in the medium, cation exchange took place and copper ions were released into the medium. *E. coli* is a facultative, anaerobic, Gram negative, rod shaped bacteria that possess adhesive fimbria and a cell wall that consists of an outer membrane containing lipopolysaccharide, a periplasmic layer with a layer of peptidoglycan and inner cytoplasmic membrane [35]. The positively charged copper ions released into the medium got attracted to the negatively charged cell membrane of bacteria by means of electrostatic interactions [36]. Oxidative damage took place and cell membrane became permeable, allowing copper ions to enter the cell and damage the DNA by releasing reactive oxygen species (ROS) [37]. The following section deals with susceptibility tests that further confirm the proposed mechanism.

3.4. Susceptibility tests of bacteria

Fig. 4(a and b) indicated the SEM images of bacteria exposed to G (0%) and GN (0.5%). There was no remarkable change in the morphology of bacteria as they were rod shaped and perfectly intact. A normal *E. coli* has an inner cytoplasmic membrane, surrounded by thin peptidoglycan layer and outer membrane containing lipopolysaccharide. Fig. 4(c and d) represented the SEM images of bacteria exposed to G (0.5%) and G (2.5%). The bacterial cell membranes were permeabilised and structural disruption has taken place. There was transformation in the structure of *E. coli* from long rod shaped to small slightly rounded structures. Small spheres of membranes called blebs were evolved from the bacteria due to rupture of cell membranes. There was aggregation of damaged bacteria. This was attributed to the release of copper ions from CAF embedded in gelatin matrix, which bound to the negatively charged cell membranes of *E. coli*. The membranes were made leaky and the vital nutrients were lost from the cell. A stream of copper ions entered the cell and damaged the genetic material by ROS generation [38].

3.5. Dissolved oxygen (DO) concentrations in CAF particles

Besides the antibacterial property, we tried to evaluate whether CAF particles were capable of increasing the DO concentration and thereby enable sufficient oxygen supply for the growth of dermal fibroblast cells. Using an LDO probe, DO concentration in

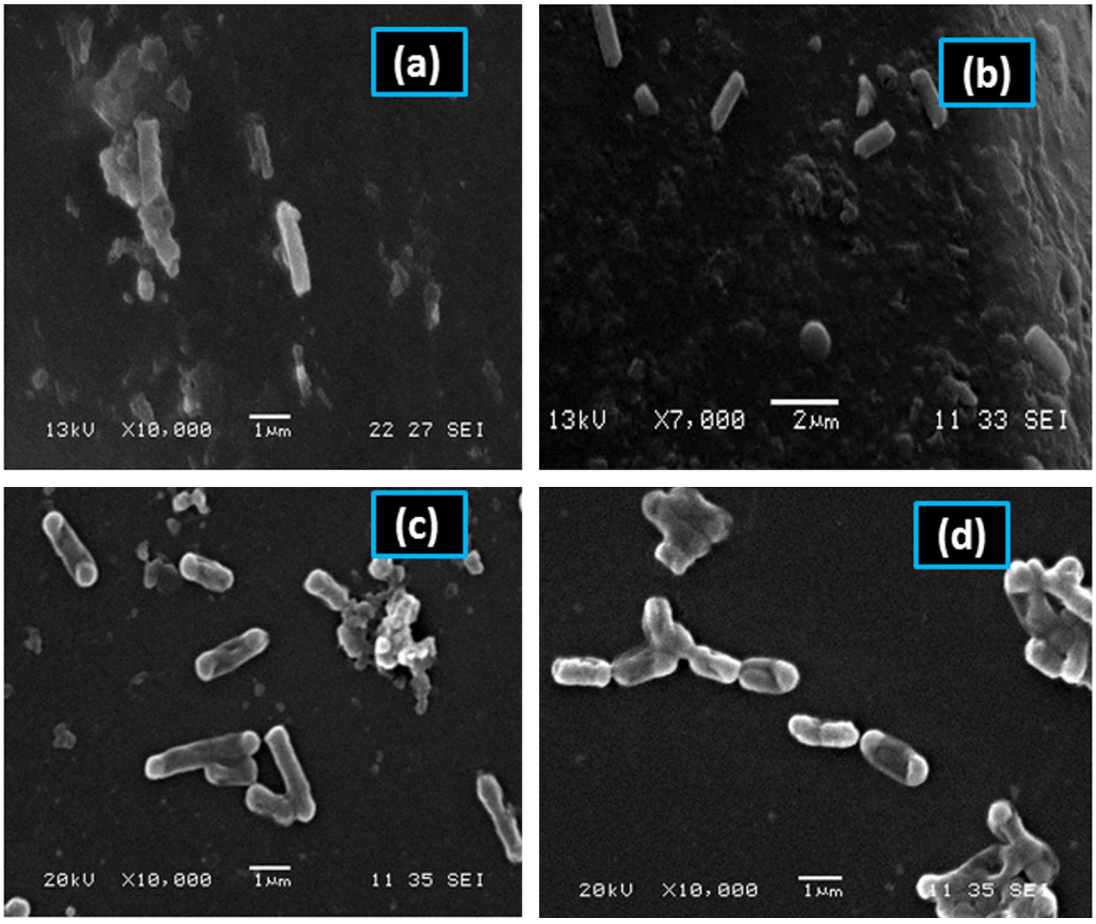

Fig. 4. SEM images of bacteria exposed to (a) G (0%) (b) GN (0.5%), (c) G (0.5%) and (d) G (2.5%), giving evidence of bacterial lysis due to copper ions released from CAF present in gelatin matrix.

the presence of different weight percentages of CAF was measured in deionised water at 37 °C and atmospheric pressure. The obtained data showed significant rise in DO concentration with increase in concentration of CAF at 37 °C compared to deionised water without any CAF particles (Fig. 5). CAF represented zeolite crystals with three dimensional pore systems. The pore diameter of CAF was 7.4 Å and the size of oxygen molecule was 1.21 Å [39]. Thus, oxygen can be easily trapped in the pores of CAF particles. They might be linked by weak Vander Waals interaction within the pores of CAF, which enabled easy diffusion of oxygen into water, obeying Henry's law [40]. Seifu et al., has reported enhanced oxygen delivery to cells seeded on scaffolds by incorporating fluorinated zeolite particles [29]. Oxygen is a vital factor for enhanced cell expansion [41]. This study reflected the potential of CAF to increase oxygen delivery to cells which promoted cell proliferation for wound healing.

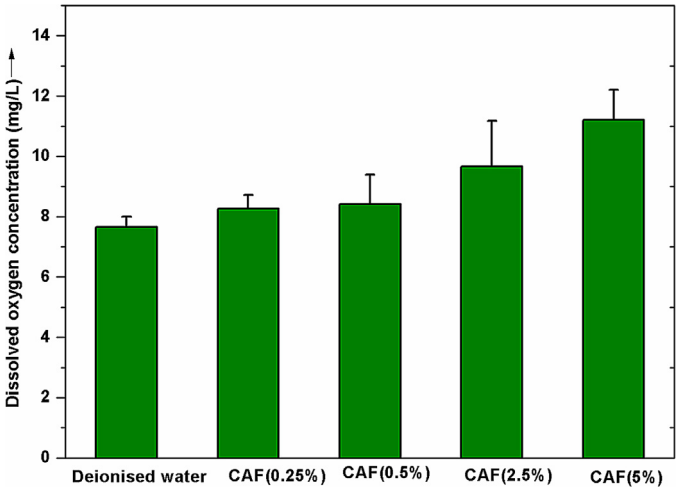

Fig. 5. Dissolved oxygen concentrations in deionised water at 37 °C in the presence of different weight percentages of copper activated faujasites particles (CAF). Values were expressed as mean ± SD ($n = 3$).

3.6. Cytocompatibility analysis

Cytotoxicity of G (0%), G (0.5%), G (2.5%) and G (5%) were assessed on NIH 3T3 fibroblast cell lines using MTS assay (Fig. 6). Among the different samples, G (0.5%) was found to have the highest cell viability (~80 ± 17%). Even though copper contained in G (0.5%) was capable of inducing bacterial lysis, it did not cause noticeable apoptosis in case of fibroblast cell lines, as eukaryotic cells show structural and functional redundancy compared to prokaryotic cells. The cell viability of G (0.5%) was higher than G (0%) due to the incorporation of CAF within the gelatin matrix, which were capable of increasing the dissolved oxygen level in cells, thereby increasing their viability. The pore size and porosity of G (0.5%) are other factors that promote fibroblast proliferation. On increasing the concentration of CAF, the viability almost decreased to 37 ± 9% and 17 ± 14%, for G (2.5%) and G (5%) respectively. Low cell viability was due to the toxic effect caused by high concentration of copper released, as analysed from the release studies. Gaetke and Chow reported about the concentration dependent toxicity induced by excess copper ions [42]. As reported in this analysis, no cytotoxic-

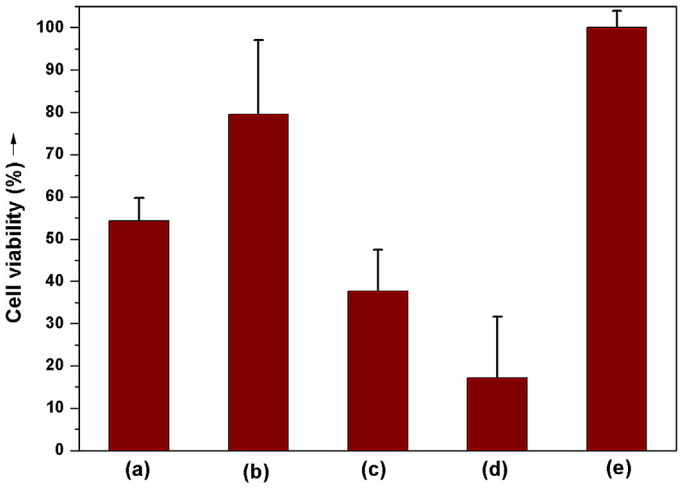

Fig. 6. Cell viability of (a) G (0%) (b) G (0.5%), (c) G (2.5%) (d) G (5%) and (e) positive control (NIH 3T3 fibroblast cells which were not exposed to samples). Values were expressed as mean ± SD ($n = 3$).

ity was observed in case of composite scaffold with 0.5% (w/w) of CAF.

3.7. In vivo studies

During the twenty days treatment period, rats showed no adverse reactions. There was no significant change in their body weight. G (0.5%) with the highest cell viability was chosen for wound healing studies. We did not notice any bleeding of granulation tissue, when scaffolds were removed from the wound site. Fig. 7A displayed the representative wound images of Group 1 rats (untreated rats) and Group 2 rats (rats treated with G (0.5%) scaffolds) on days 0, 4, 8, 12, 16 and 20. Fig. 7B showed the percentage reduction in wound area during 20 days. The wounds of Group 1 rats were healed only after 34 days. On day 20, the wounds of Group 2 rats were significantly smaller ($p < 0.5$) than Group 1 rats. Group 2 rats demonstrated 93 ± 3% reduction in wound area on day 20 whereas Group 1 rats showed only 69 ± 2% reduction. Cell migration was observed from both sides of the wound towards the centre which resulted in reduction in wound size.

3.8. Histological assessment of wound healing

The histological examination of H&E stained skin sections on day 3 and day 20 were shown in Fig. 8. It was found that the inflammatory phase of Group 1 rats was prolonged compared to Group 2 rats. In case of Group 1 rats, the level of inflammation was intensified on day 3 compared to Group 2 rats. The presence of red blood cells (RBC) due to rupture of blood vessels and various leukocytes at the wound site were evidences to support this statement. On the other hand, in case of Group 2 rats, along with inflammatory cells, fibroblasts were observed which proved that length of inflammatory phase was comparatively less.

On day 20, scab tissue was found in case of Group 1 rats beneath which the epidermal layers were growing. Complete re-epithelialisation did not take place. There were white empty spaces in the dermis due to poor collagen deposition. On the other hand, complete re-epithelialisation was observed in case of Group 2 rats with well-developed epidermal and dermal layers. The absence of scab tissue and the presence of rete peg formation confirmed

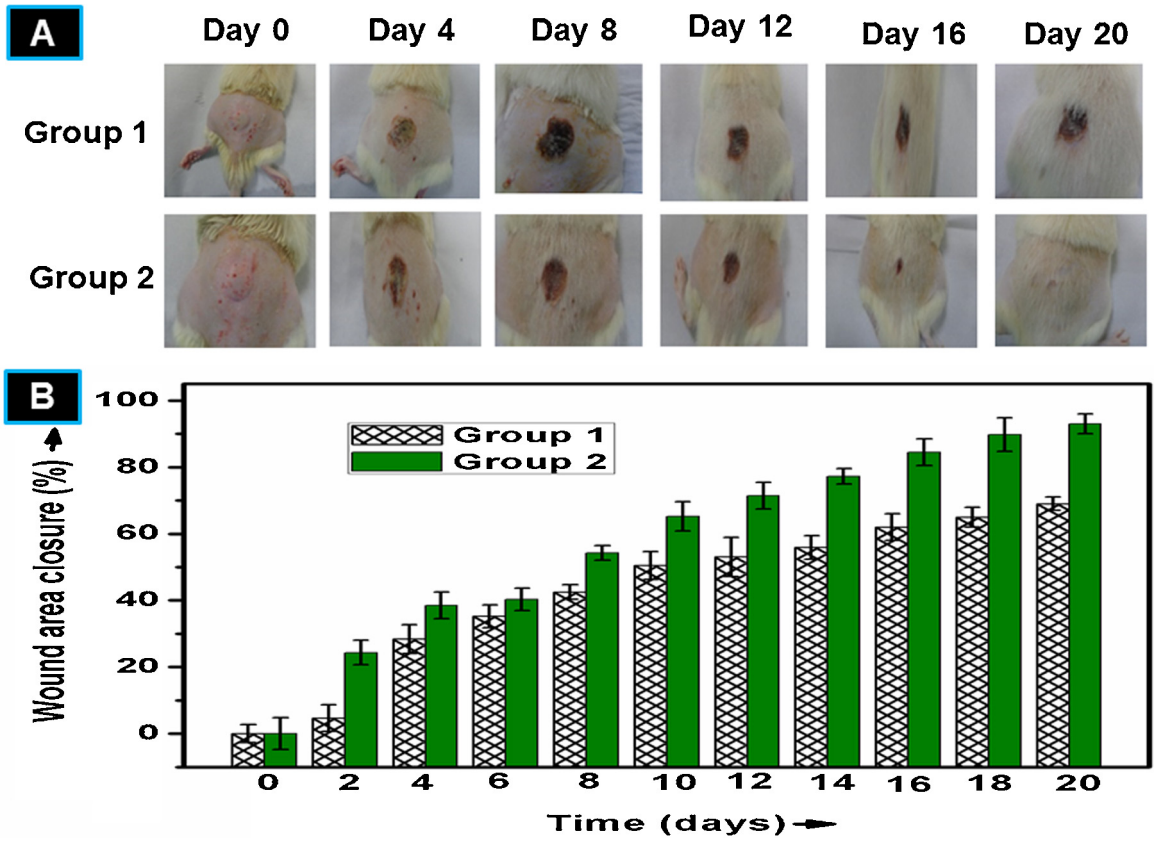

Fig. 7. (A) Macroscopic pictures of wounds of control rats (Group 1) and rats are treated with G (0.5%), (Group 2) for 20 days. (B) Assessment of wound area closure. All data reported as mean ± SD ($n = 3$), $^{*}p < 0.05$.

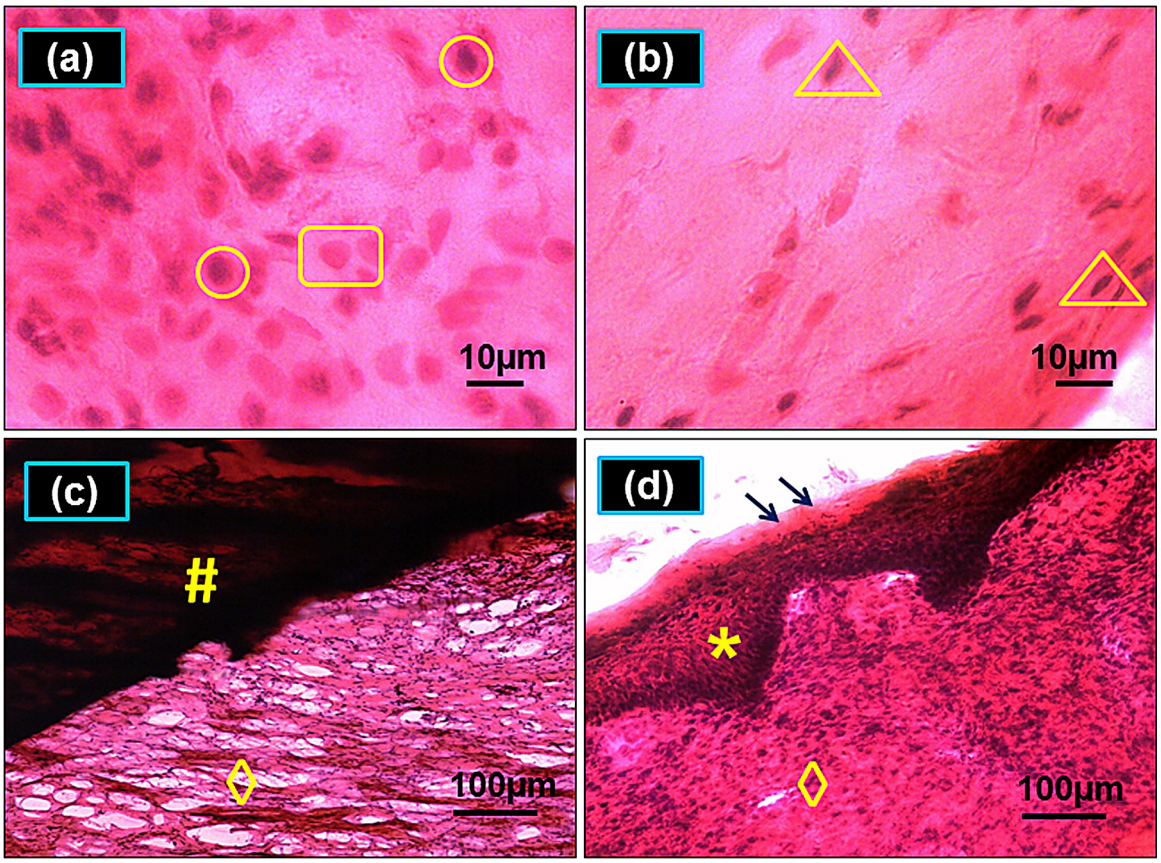

Fig. 8. Photomicrographs of haematoxylin and eosin stained wound tissue on (a) Group 1 and (b) Group 2 during inflammatory phase; (c) Group 1 and (d) Group 2 on day 20. (The symbols like, (○) denoted eosinophils, (△) referred to fibroblasts, (□) represented RBC, (#) showed scab tissue, (◊) indicated dermis, (*) suggested rete peg formation and (↓) indicated stratum corneum.)

that they were in the re-modelling phase. There was good collagen deposition in the dermis and keratinocyte infiltration in the epidermis. Thus, G (0.5%) exhibited positive wound healing profile. The enhanced oxygen supply and antibacterial effect of CAF might have facilitated skin regeneration and neovascularisation.

4. Conclusion

In this work, we successfully prepared gelatin/CAF composite scaffold by lyophilisation. The prepared composite scaffold showed antibacterial properties due to copper leached from the core of faujasite. It demonstrated high viability on NIH 3T3 fibroblast cell lines. It was also found that the dissolved oxygen concentration got significantly increased in the presence of CAF, showing its potential to meet the oxygen demands of growing skin fibroblast cells. Finally, the results proved that G (0.5%) present a potentially viable matrix for partial thickness wound healing in a mouse model. Thus, G (0.5%) is an ideal tissue engineering scaffold which displayed antibacterial and wound healing properties.

Acknowledgements

We are thankful to Brittany region, The European Union (FEDER) and the French Ministry for research for rendering financial support for conducting the studies.

References

[1] R. Jayakumar, M. Prabaharan, P.T. Sudheesh Kumar, S.V. Nair, H. Tamura, Biotechnol. Adv. 29 (2011) 322–337.
[2] N. Ninan, S. Thomas, A. George, M. Sebastian, Ther. Deliv. 2 (2011) 711–715.
[3] H. Tlaskalová-Hogenová, R. Štěpánková, T. Hudcovic, L. Tučková, B. Cukrowska, R. Lodinová-Žádní′ková, H. Kozáková, P. Rossmann, J. Bártová, D. Sokol, D.P. Funda, D. Borovská, Z. Řeháková, J. Šinkora, J. Hofman, P. Drastich, A. Kokešová, Immunol. Lett. 93 (2004) 97–108.
[4] K. Madhumathi, P.T. Sudheesh Kumar, S. Abhilash, V. Sreeja, H. Tamura, K. Manzoor, S.V. Nair, R. Jayakumar, J. Mater. Sci.: Mater. Med. 21 (2010) 807–813.
[5] N. Ninan, M. Muthiah, I.-K. Park, A. Elain, S. Thomas, Y. Grohens, Carbohydr. Polym. 98 (2013) 877–885.
[6] P.T.S. Kumar, S. Abhilash, K. Manzoor, S.V. Nair, H. Tamura, R. Jayakumar, Carbohydr. Polym. 80 (2010) 761–767.
[7] H.-D. Wu, D.-Y. Ji, W.-J. Chang, J.-C. Yang, S.-Y. Lee, Mater. Sci. Eng. C: Mater. Biol. Appl. 32 (2012) 207–214.
[8] C.-W. Peng, H.-Y. Lin, H.-W. Wang, W.-W. Wu, Mater. Sci. Eng. C: Mater. Biol. Appl. 32 (2012) 2491–2500.
[9] A. Mandal, V. Meda, W.J. Zhang, K.M. Farhan, A. Gnanamani, Colloids Surf. B: Biointerfaces 90 (2012) 191–196.
[10] M. Kharaziha, M. Nikkhah, S.-R. Shin, N. Annabi, N. Masoumi, A.K. Gaharwar, G. Camci-Unal, A. Khademhosseini, Biomaterials 34 (2013) 6355–6366.
[11] S. Balaji, R. Kumar, R. Sripriya, P. Kakkar, D.V. Ramesh, P.N.K. Reddy, P.K. Sehgal, Mater. Sci. Eng. C: Mater. Biol. Appl. 32 (2012) 975–982.
[12] C. Yao, X. Li, K.G. Neoh, Z. Shi, E.T. Kang, J. Membr. Sci. 320 (2008) 259–267.
[13] M.A. Fanovich, J. Ivanovic, D. Misic, M.V. Alvarez, P. Jaeger, I. Zizovic, R. Eggers, J. Supercrit. Fluid. 78 (2013) 42–53.
[14] Y. Mei, C. Yao, K. Fan, X. Li, J. Membr. Sci. 417/418 (2012) 20–27.
[15] A. Hashemi Doulabi, H. Mirzadeh, M. Imani, N. Samadi, Carbohydr. Polym. 92 (2013) 48–56.
[16] P. Kaali, E. Strömberg, R.E. Aune, G. Czél, D. Momcilovic, S. Karlsson, Polym. Degrad. Stab. 95 (2010) 1456–1465.
[17] L. Dreesmann, M. Ahlers, B. Schlosshauer, Biomaterials 28 (2007) 5536–5543.
[18] R.E. Gámez Sazo, K. Maenaka, W. Gu, P.M. Wood, M.B. Bunge, Biomaterials 33 (2012) 8529–8539.
[19] P.-o. Rujitanaroj, N. Pimpha, P. Supaphol, Polymer 49 (2008) 4723–4732.
[20] S. Thilagar, N.A. Jothi, A.R.S. Omar, M.Y. Kamaruddin, S. Ganabadi, J. Biomed. Mater. Res. B: Appl. Biomater. 88B (2009) 12–16.
[21] M. Peter, N. Ganesh, N. Selvamurugan, S.V. Nair, T. Furuike, H. Tamura, R. Jayakumar, Carbohydr. Polym. 80 (2010) 687–694.
[22] X. Zhuang, B. Cheng, W. Kang, X. Xu, Carbohydr. Polym. 82 (2010) 524–527.
[23] J. Gil-Albarova, M. Vila, J. Badiola-Vargas, S. Sánchez-Salcedo, A. Herrera, M. Vallet-Regi, Acta Biomater. 8 (2012) 3777–3783.

[24] Y. Zhou, Y. Zhao, L. Wang, L. Xu, M. Zhai, S. Wei, Radiat. Phys. Chem. Oxf. Engl. 1993 81 (2012) 553–560.
[25] J. Wang, Z. Wang, S. Guo, J. Zhang, Y. Song, X. Dong, X. Wang, J. Yu, Microporous Mesoporous Mater. 146 (2011) 216–222.
[26] C. Wu, Y. Zhou, M. Xu, P. Han, L. Chen, J. Chang, Y. Xiao, Biomaterials 34 (2013) 422–433.
[27] N. Ninan, M. Muthiah, I.-K. Park, A. Elain, T.W. Wong, P.S. Thomas, Y. Grohens, ACS Appl. Mater. Interfaces 5 (2013) 11194–11206.
[28] P. Kumar, C.-Y. Sung, O. Muraza, M. Cococcioni, S. Al Hashimi, A. McCormick, M. Tsapatsis, Microporous Mesoporous Mater. 146 (2011) 127–133.
[29] D.G. Seifu, T.T. Isimjan, K. Mequanint, Acta Biomater. 7 (2011) 3670–3678.
[30] N. Ninan, Y. Grohens, A. Elain, N. Kalarikkal, S. Thomas, J. Eur. Polym. 49 (2013) 2433–2445.
[31] T.-W. Wang, J.-S. Sun, H.-C. Wu, Y.-H. Tsuang, W.-H. Wang, F.-H. Lin, Biomaterials 27 (2006) 5689–5697.
[32] K.A. Almeida, R. Landers, D. Cardoso, J. Catal. 294 (2012) 151–160.
[33] J.J. Liu, Y. Kim, F. Yan, Q. Ding, V. Ip, N.N. Jong, J.F.B. Mercer, M.J. McKeage, Biochem. Pharmacol. 85 (2013) 207–215.
[34] B.-L. Wang, X.-S. Liu, Y. Ji, K.-F. Ren, J. Ji, Carbohydr. Polym. 90 (2012) 8–15.
[35] M.S. Harper, C. Carpenter, D.J. Klocke, G. Carlson, T. Davis, B. Delaney, Food Chem. Toxicol. 49 (2011) 1770–1772.
[36] S. Cometa, R. Iatta, M.A. Ricci, C. Ferretti, E. De Giglio, J. Bioact. Compat. Polym. 28 (2013) 508–522.
[37] C. Manzl, J. Enrich, H. Ebner, R. Dallinger, G. Krumschnabel, Toxicology 196 (2004) 57–64.
[38] A. Pramanik, D. Laha, D. Bhattacharya, P. Pramanik, P. Karmakar, Colloids Surf. B: Biointerfaces 96 (2012) 50–55.
[39] V.I. Sobolev, K.Y. Koltunov, J. Mol. Catal. A: Chem. 347 (2011) 22–27.
[40] E. Schuhfried, F. Biasioli, E. Aprea, L. Cappellin, C. Soukoulis, A. Ferrigno, T.D. Märk, F. Gasperi, Chemosphere 83 (2011) 311–317.
[41] M. Lönne, A. Lavrentieva, J.-G. Walter, C. Kasper, Cell Tissue Res. (2013) 1–6.
[42] L.M. Gaetke, C.K. Chow, Toxicology 189 (2003) 147–163.